

# Nanometre scale textures in agate and Beltane opal

LU TAIJING AND X. ZHANG

Department of Physics, National University of Singapore, Lower Kent Ridge Road, Singapore 0511

ICHIRO SUNAGAWA

Yamanashi Institute of Gemology and Jewelry Arts, Tokoji-machi, 1955-1, Kofu, Yamanashi, 400 Japan

G. W. GROVES

Department of Materials, University of Oxford, Parks Road, Oxford OX1 3PH, UK

## Abstract

We have carried out TEM observations of agates of geode origin and Beltane opals. Optically observable individual fibres in agates are composed of many fine fibres which consist of quartz crystallites of 8 to 100 nm in length stacked together parallel to  $\langle 11\bar{2}0 \rangle$  or  $\langle 1\bar{1}00 \rangle$  with  $c$ -axes perpendicular to the fibre elongation. The optically observable systematic striations in agate are found to consist of cyclic alternation of layers due to variation in grain size and porosity. Large quartz crystals, protruding into the spaces of geodes, represent the last stage of formation of these bands, and are merely a continuation of the banding sequence. Nanometre scale textures of cristobalite fibres were revealed in Beltane opals. The cristobalite crystallites have the size of 3 to 20 nm in length and are also stacked together. Our TEM results suggest that embryonic particles were formed in their corresponding growth environments and agglutinated to form fibres.

KEYWORDS: agate, opal, texture, TEM observation, fibre.

## Introduction

FIBROUS texture is ubiquitous in concentrically banded (lining-type) agate layers of geode origin. It has been investigated extensively since the last century (e.g. Brewster 1843; Liesegang, 1915; Copisarow and Copisarow, 1942; Frondel, 1962, 1978; Ball and Burns, 1975; Sunagawa and Ohta, 1976; Graetsch *et al.*, 1987). In the optical microscope, the fibrous texture varies in appearance, forming parallel or subparallel aggregates, bundles of fibres, sheaf-like, divergent, leafy aggregates of fibres or spherulites (Frondeb, 1978). The direction of the fibre elongation is determined by polarized light and this result is confirmed by X-ray and piezoelectric techniques to be  $\langle 10\bar{1}0 \rangle$  or  $\langle 11\bar{2}0 \rangle$  (Frondeb, 1962; Correns and Nogelschmidt, 1933;

Braitsch, 1957). Using transmission electron microscopy (TEM), Miede *et al.* (1984) and Graetsch *et al.* (1987) observed submicroscopic polysynthetic twinning of right- and left-handed lamellae in quartz crystals in agate. Two of the present authors (Lu and Sunagawa, 1994) examined agate using TEM and reported the fibrous textures in lining-type agate layers of geode origin. Compared to agate, only in few cases are fibrous textures observed optically in Beltane opal, since Beltane opal usually displays complex textures with optical unresolvable micro-textures. Two of the present authors (Groves *et al.*, 1987; Zhang *et al.*, 1990.) examined Beltane opal using TEM and reported the existence of fibrous textures.

It is the aim of this paper to study nanometre scale textures revealed in agate and Beltane opal using TEM.

We observed nanometre scale textures in both quartz fibres from agates and cristobalite fibres from Beltane opal. These results suggest the formation of the fibres may have resulted from the agglutination of nanometre scale embryonic particles existing in the solutions.

### Samples

Samples used in the present study are geode origin agate from Uruguay, Brazil, Japan (Fukushima) and China (Jangsu) and opal from the USA (Beltane, California). Particular attention has been paid to establishing a correlation between optically observable textures and electron microscopic textures. TEM observation was made using a JEOL 1MV instrument (Tohoku University) and an AEI 1MV instrument (Oxford University). The high-voltage TEM was used because it gives less electron beam damage than conventional TEM and it has strong transmission ability, by which a wide area can be easily examined; it is then easier to study the correlations between optically observable textures and electron microscopic observations. Thin (30  $\mu\text{m}$ ) sections, diamond-polished on both sides were used for transmitted polarized light microscopy. TEM specimens were prepared by choosing suitable areas from the thin sections and then further thinning by etching with Ar-ions using Edward's or Gatan instruments. Preparation of a good quality TEM specimen usually takes several days. Etching experiments with HF solutions and powder X-ray diffraction analysis techniques were also used to confirm the results.

### Observations

Under transmitted light polarization microscopes, the width of the fibres ranges from 1 to 50  $\mu\text{m}$  and the lengths from 5  $\mu\text{m}$  to 2 mm depending on the specimens and the positions in the specimen. The width-to-length ratio ranges from 1:10 to 1:300. Further away from the geode wall, divergent or hemispherical aggregates of fibres tend to become less distinct. Essential points obtained in our TEM observations are summarized as follows:

(a) The optically observable fibres (Fig. 1a) are composed of much finer and nearly parallel fibres as shown in Fig. 1b which is a TEM photomicrograph of the selected area A in Fig. 1a. The finer fibres have the same elongation as optically observable fibres. There is a proportional relationship between the widths of optically observable fibres and finer fibres seen by TEM. Wider fibres observed by optical microscope are generally composed of wider fine fibres visible in the TEM. One optically observable fibre usually consists of 10 to 50 finer fibres.

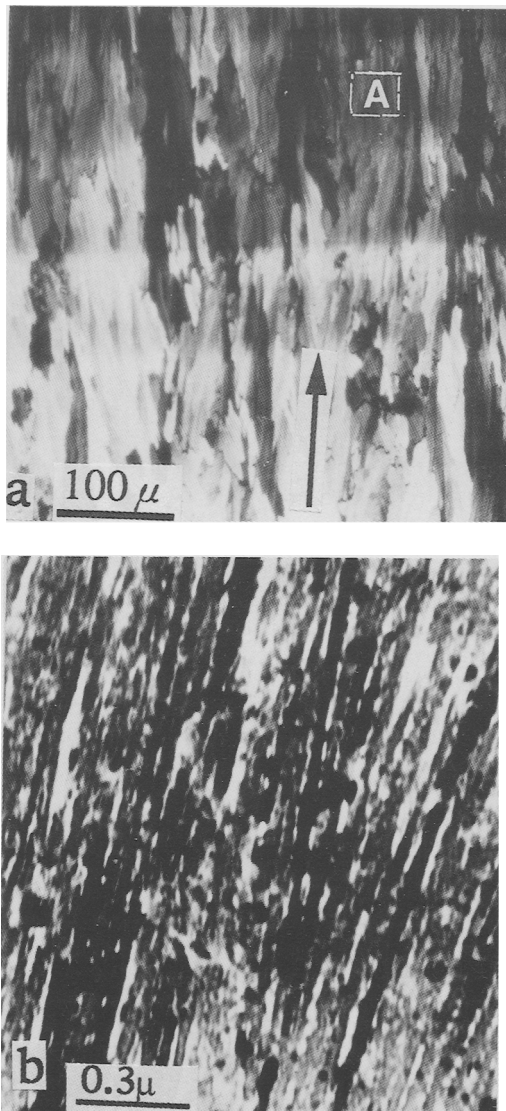


Fig. 1. (a) Polarized light photomicrograph of lining type agate showing optically observable fibrous texture (Arrow indicating the elongation direction of the fibres). (b) TEM photomicrograph of the area indicated by letter A in (a) showing that the fibres in (a) consist of many parallel nanometre scale fibres.

(b) Each fine fibre is composed of a large number of tiny quartz crystallites with slightly elongated and anhedral morphology. Their sizes range from 8 to 100 nm in length. From dark-field diffraction contrast images with one of the  $\langle 11.0 \rangle$  spots as the operating

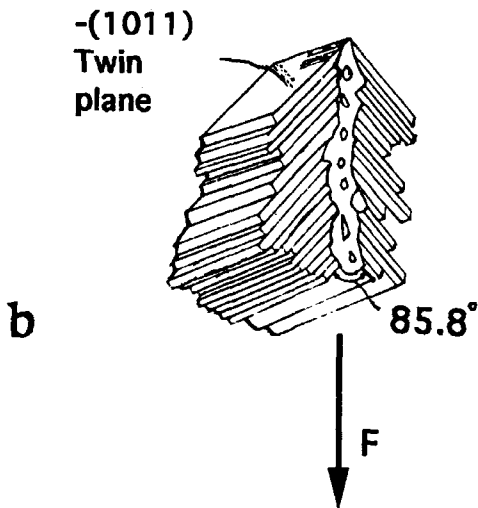
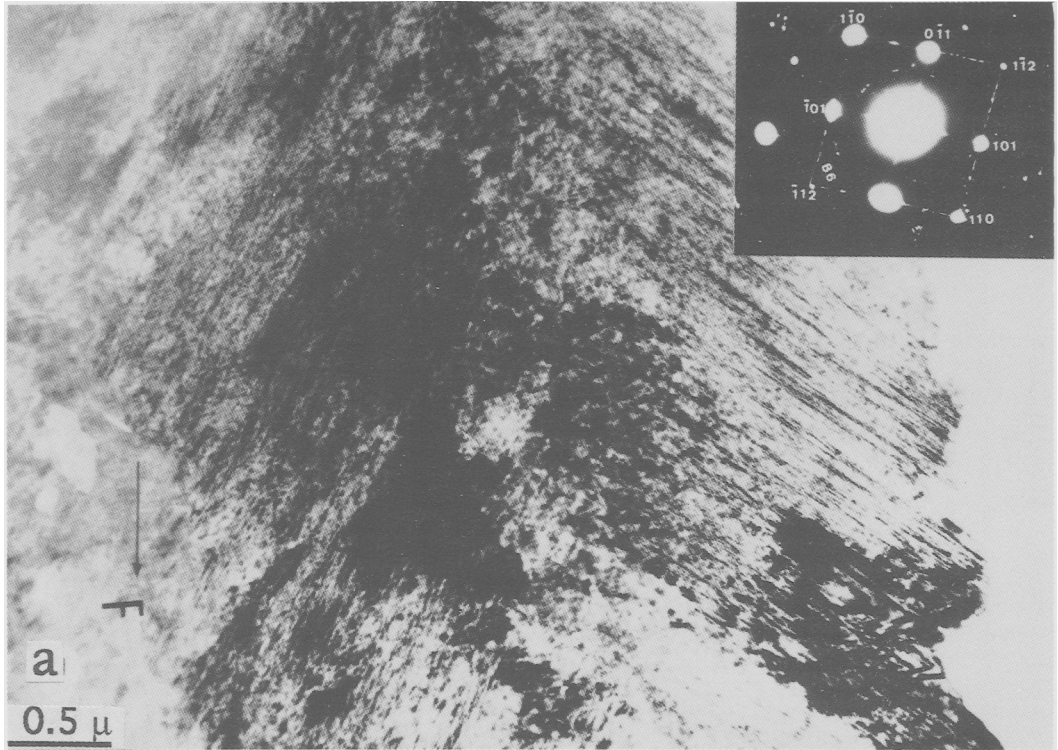


FIG. 2(a) TEM photomicrograph of agate showing two systems of Brazil twin boundaries observed in a relatively large grain together with the corresponding diffraction pattern (upper right) of selected area A in the picture. (b) Schematic representation of (a) showing the relationships of the orientations between the Brazil twin boundaries and the elongation of the optically observable fibres (F).

reflection it was confirmed that the tiny quartz crystallites are arranged roughly along the orientation of  $\langle 1120 \rangle$  or  $\langle 10\bar{1}0 \rangle$  in individual fine fibres, with

the  $c$ -axes perpendicular to the fibre elongation. The other crystallographic axes of the tiny quartz crystals are slightly different from each other in the fine fibre.

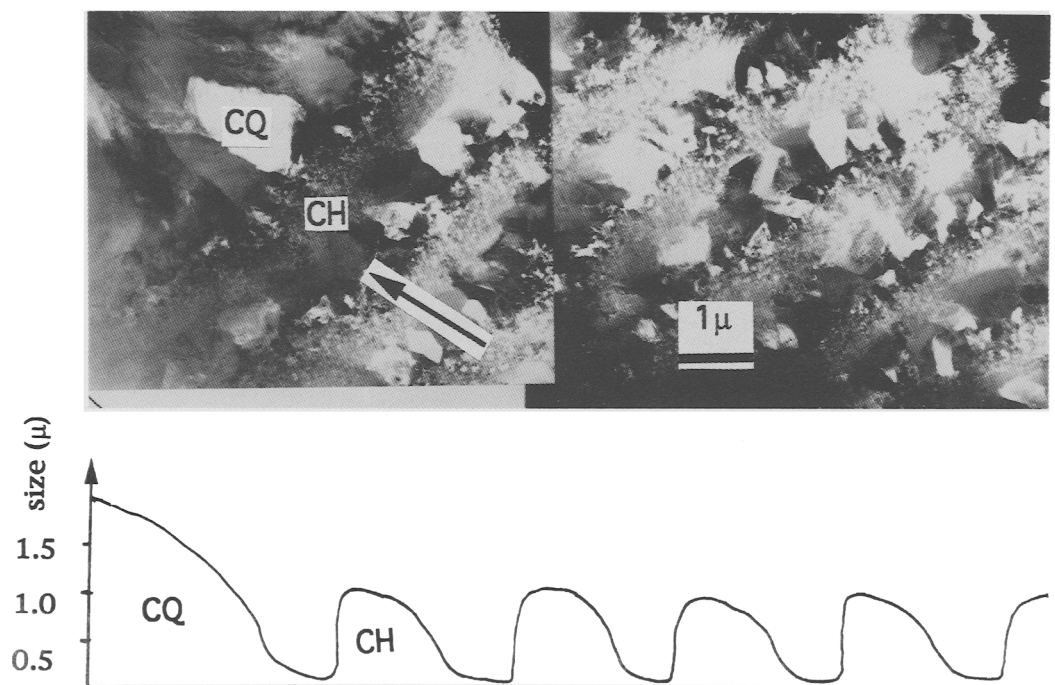


FIG. 3. A mosaic TEM photomicrograph showing that the optically observable systematic striations are composed of alternating coarse and fine grains of quartz. Note the size of grains increases gradually from the beginning to the end of a layer along the direction toward the geode centre (arrow direction) in each striation. CH means chalcedony and CQ means coarse quartz crystals occurring in the centre of the geode. The variation of grain size is schematically shown below.

The orientations of the neighbouring fine fibres are slightly different as well.

(c) In the optically observable fibres with widths of more than about 30  $\mu\text{m}$ , two sets of thin lamellae parallel to  $\{10\bar{1}1\}$  are usually observed. An example is shown in Fig. 2a. The thickness of the lamellae is 10–30 nm. On the selected area electron diffraction pattern, streaks of diffuse intensity in  $\langle 10.1 \rangle$  directions with maxima at  $h \pm \frac{1}{2}, k, l \pm \frac{1}{2}$ , are observed (see inserted ED pattern in Fig. 2a). These results indicate that the thin lamellae are polysynthetic Brazil twin lamellae (Miehe *et al.*, 1984). The orientational relationship between Brazil twin lamellae and the fibre elongation is schematically shown in Fig. 2b. Along the intersection of two sets of Brazil twin lamellae, small pores and solid inclusions are observed.

(d) Towards the central space of a geode where large quartz or amethyst crystals occur, fibrous textures become less pronounced and almost uniformly spaced systematic striations are often seen by optical microscope (Fron del, 1962, 1978.). Our observations show that the striations are

composed of cyclic alternations of layers. The grain size and porosity in each layer have similar variations from the beginning to the end of each layer in the direction towards the centre of the geode. The quartz grain size and the porosity increase gradually from the beginning to the end of each layer and decrease sharply at the beginning of the next layer. The minimum size of a quartz crystallite at the beginning of a layer is 6 nm, and the maximum size at the end of the layer is about 1.5  $\mu\text{m}$  (Fig. 3). The size difference between the beginning and end sites in each striation is of the order of power 2 to 3, although the maximum and minimum sizes may vary from specimen to specimen. As the size of the tiny quartz crystallite increases the orientations of the grains become relatively random and the grains display irregular morphologies. It was also found that the same sequence from smaller to larger grains continues up to the coarse quartz crystals (CQ) at the topmost surface of the last systematic striation. Therefore, coarsely crystalline quartz lining the cavity at the centre of the geode is merely a continuation of the systematic striations and

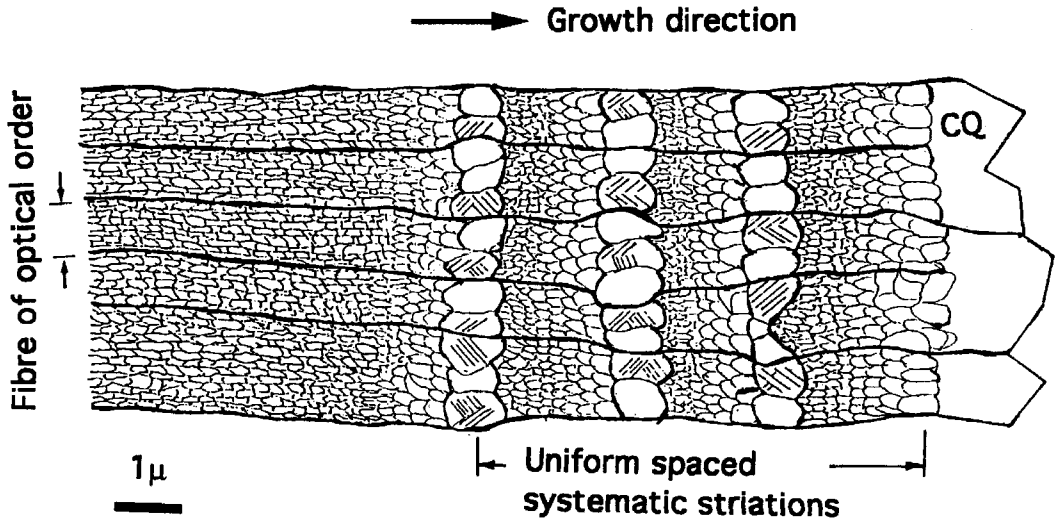


FIG. 4. Schematic drawing illustrating the relationships among optically observable fibrous texture, electron microscopically observable fibres, uniformly-spaced systematic striations observed in lining type agate and coarse quartz (CQ) in agate geode.

represents the last stage of their formation. The relationships between optically observable fibres, electron microscopically observable fibres, systematic striations and coarse quartz in geode agate are shown schematically in Fig. 4.

Beltane opal shows a complex structure consisting of core and rim portions under the transmitted light polarization microscope. Single quartz grains with sizes of one to a few  $\mu\text{m}$  form the cores, whereas the rim portions usually have optically unresolved microstructures. The opal contains about 15% quartz core. Our TEM observation revealed the following fine textures.

(a) Fine fibres with varying sizes predominate the rim portions. Their electron beam diffraction pattern showed their structures to be disordered cristobalite. A typical area is shown in Fig. 5. A diffuse diffraction ring corresponding to a  $d$ -spacing of approximately 0.4 nm is characteristic of this material and is more readily recognized in selected area electron diffraction. The diffuse ring sometimes contains spots which appear to originate from the largest fibres, indicating that the largest fibres may have a relatively ordered structure. The smallest fibres are formed of particles of a few nm to a few tens of nm in diameter with roughly circular cross-sectional shape that appear to be non-crystalline. It is difficult to determine the degree of the crystallinity of these smallest fibres since they are too small to get reliable corresponding diffraction patterns.

(b) Some large relatively perfect quartz crystals with a size from a few tens of nm to a few  $\mu\text{m}$  were also observed. Some of them correspond to the quartz

crystals observed under the optical microscope. The quartz crystals generally have irregular morphologies and are surrounded by a region consisting of disordered cristobalite grains. These disordered cristobalite grains usually appear densely packed and have sizes of less than 10 nm with non-distinctive form. The cristobalite fibres appear in the regions with free spaces such as pores in the opal. It is also found that when the fibres are close to the free space, they are stacked nearly parallel to each other and fibres become bigger. The relationship between large quartz crystals, dense disordered cristobalite layer and cristobalite fibres in a complex texture is shown diagrammatically in Fig. 6.

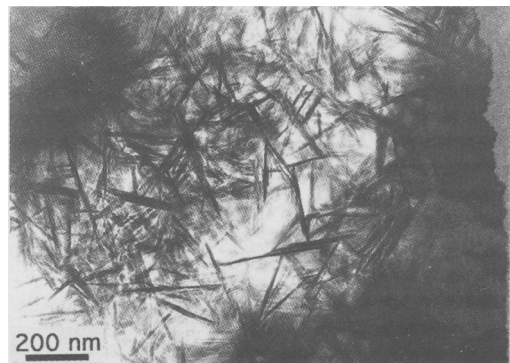


FIG. 5. TEM photomicrograph of the rim portion of Beltane opal observed under optical microscope showing nanometre scale cristobalite fibres.

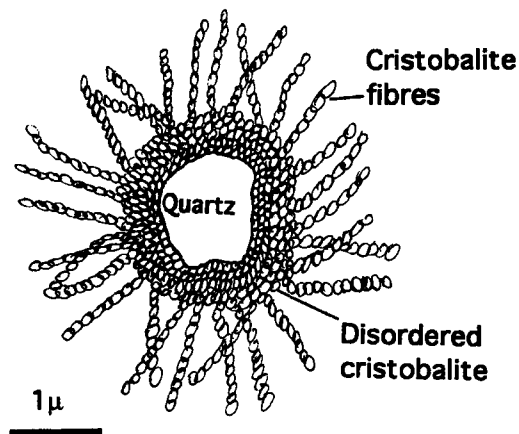


FIG. 6. Schematic drawing to show the relationship among a large quartz crystal, the dense disordered cristobalite layer and cristobalite fibres in a complex texture of Beltane opal.

### Discussion

Although agate of geode origin and Beltane opal are formed under different conditions, it is noted that nanometre scale textures are observed by TEM in both cases. In agate, the fine fibres consist of nanometre sized quartz grains which are stacked in strings in nearly the same crystallographic orientation. In Beltane opal, the fibres are composed of nanometre sized cristobalite grains which are stacked together. The fibres form the rims of the core-rim textures observed by optical microscope. Such nanometre scale textures have not been reported and compared previously. Unless we assume that the individual embryonic particles of nanometre size nucleated initially in both types of formation environment and then agglutinated and developed to form fibres, it is difficult to explain the observed textures. If a fibre is formed as a single crystal through incorporation of ionic entities, the fibre would not show the observed nanometre scale textures. The present observations suggest that the solution from which the agate and Beltane opal precipitated contained nanometre sized polymerized particles, and the formation of agate and Beltane opal proceeded through agglutination of these particles, although we still do not know the driving force for such agglutination.

The fibrous texture in agate becomes less distinct towards the later stages of agate formation, or further away from the geode wall. In such zones systematic striations are seen, which appear due to grain size distribution. This suggests that within each band the crystallization conditions became more stable and the

growth rates were slowed down away from the geode wall. In contrast, more fluctuating conditions and higher growth rates should be inferred during the early stage of agate formation in the geode where fibrous textures are more distinct. Although at present we do not know the driving force to agglutinate nanometre size crystallites in more or less ordered orientations, we may mention electrophoresis as a plausible cause.

### Conclusions

Optically observable individual fibres in concentrically banded (lining-type) agates of geode origin are composed of much finer fibres, in which quartz crystallites of 8 to 100 nm in length are stacked together parallel to  $\langle 11\bar{2}0 \rangle$  or  $\langle 10\bar{1}0 \rangle$ . Brazil twin lamellae structures are frequently observed in grains larger than 30 nm in length. Uniformly spaced systematic striations consist of a cyclic alternation in quartz grain sizes, with the smallest sizes of 6 nm. Coarse quartz or amethyst crystals radiating inward from agate banding appear to be a continuation of the sequence of systematic striations and the appearance of coarse quartz or amethyst represent the final stage of agate (lining-type) formation.

Fine fibrous textures observed in Beltane opal are composed of cristobalite crystallites with sizes of 8 to 20 nm stacked together. They appear as the rims surrounding quartz crystals, and grow into regions with free space.

The observation of nanometre sized textures suggest the presence of embryonic polymerized particles in the solution, which agglutinate to form fibres, possibly driven by electrophoresis.

### Acknowledgements

One of the authors (Lu) expresses his thanks to Prof. M. Akizuki, Tohoku University for his encouragement.

### References

- Ball, R. A. and Burns, R. L. (1975) *Austral. Gemol.*, **12**, 143–50.
- Braitsch, O. Y. (1957) *Beitr. Mineral. Petrogr.*, **5**, 331–72.
- Brewster, D. (1843) *Philos. Mag.*, **22**, 434–5.
- Copisarow, A. C. and Copisarow, M. (1942) *Nature*, **149**, 413.
- Correns, C. W. and Nagelschmidt, G. (1933) *Zeits. Kristallogr.*, **85**, 199–213.
- Fron del, C. (1962) *The System of Mineralogy, Vol. III, Silica Minerals*. Seventh Edition, New York, Wiley.
- Fron del, C. (1978) *Amer. Mineral.*, **63**, 17–27.

- Graetsch, H., Florke, O. W. and Mische G. (1987) *Phys. Chem. Minerals*, **14**, 247–9.
- Groves, G. W., Hodges, D. J. and Zhang, X. (1987) *Proc. 9th Intern. Conf. on Cement Microscopy, Reno, USA*, 458–65.
- Liesegang, R. E. (1915) *Die Achate*, Dresden Ce, Leipzig (Th. Steinkopff).
- Lu Taijing and Sunagawa, I. (1994) *Mineral J.*, **17**, 53–76.
- Mische, G., Graetsch, H. and Florke, O. W. (1984) *Phys. Chem. Minerals*, **10**, 197–9.
- Sunagawa, I. and Ohta, E. (1976) *Sci. Rep., Tohoku Univ.*, **13**, 131–46.
- Zhang, X., Blackwell, B. Q. and Groves, G. W. (1990) *Brit. Ceram. Trans. J.*, **89**, 899–92.
- [Manuscript received 22 March 1994:  
revised 10 June 1994]